

Supporting Information

A fluorescent naphthalimide NADH mimic for continuous and reversible sensing of cellular redox state

Hemant Sharma,^a Nian Kee Tan,^b Natalie Trinh,^b Jia Hao Yeo,^b Elizabeth J. New^b and Frederick M. Pfeffer*^a

^aSchool of Life and Environmental Sciences, Deakin University, Waurn Ponds, VIC 3216, Australia.

^bSchool of Chemistry, The University of Sydney, Sydney, NSW 2006, Australia.

E-mail: fred.pfeffer@deakin.edu.au.

Contents:

S1 Synthesis	2
S2 Spectra of new compounds	4
S3 UV-vis and fluorescence spectroscopy experiments	7
S4 Electrochemistry	11
S5 Additional ¹ H NMR experiments	12
S6 Imaging	13
S7 Comparison of NapNic with related probes	16
References	17

S1 Synthesis

S1.1 General

All reagents and solvents were obtained from commercial suppliers and used as supplied. All NMR studies were performed on Bruker Avance 400 MHz or 500 MHz spectrometer as specified. NMR spectra were recorded in deuterated solvent DMSO-*d*₆. Spectra are reported as chemical shift (integration, multiplicity, coupling constant (*J*) values in Hertz (Hz) and assignment). Melting points are recorded on Bibby Stuart Scientific SMP3 melting point apparatus and reported without correction. High resolution mass spectral data was recorded using an AB SCIEX TripleTOF 5600 mass spectrometer in a 95% MeOH:H₂O solvent system containing 0.1% formic acid. Samples were prepared in HPLC grade methanol (~1 mg mL⁻¹).

Microwave reactions were performed using a CEM Discover S-Class Microwave reactor, operating at a frequency of 50/60 Hz and continuous irradiation power from 0 to 200 W. Reactions were performed in a 35 mL microwave vial sealed with a Teflon® crimp cap.

The G3-Xantphos catalyst was prepared using the procedure reported by Carole *et. al.*¹

S1.2 Synthesis of probe 4

6-Bromo-2-propyl-1*H*-benzo[*de*]isoquinoline-1,3(2*H*)-dione **2**^{2,3}

Compound **2** was synthesised according to our reported procedure.³ In brief, a mixture of 4-bromo-1,8-naphthalic anhydride (3.057 g, 11.03 mmol) and propylamine (950 μL, 11.56 mmol) was dissolved in ethanol (15 mL). The reaction was heated using microwave irradiation at 100 °C for 1 h. Afterwards, the reaction mixture was poured into H₂O and cooled to 0 °C. The resulting precipitate was collected using vacuum filtration followed by washing with H₂O. ¹H NMR data matched the reported data.^{2,3}

N-(1,3-Dioxo-2-propyl-2,3-dihydro-1*H*-benzo[*de*]isoquinolin-6-yl)-nicotinamide **3**

Compound **3** was synthesised using a slight modification of our previously reported methodology for the related *N*-(2-methoxy)ethyl imide³ and involved a one-step amidation of 4-bromo-1,8-naphthalimide **2** with nicotinamide.

A mixture of bromonaphthalimide **2** (200 mg, 0.63 mmol), nicotinamide (115 mg, 0.94 mmol, 1.5 equiv.), Cs₂CO₃ (308 mg, 0.94 mmol, 1.5 equiv.), G3-Xantphos (12 mg, 0.014 mmol, 0.02 equiv.) and 1,4-dioxane (2.5 mL) were combined in oven dried flask. The resultant mixture was heated at 100 °C for 2 h under N₂. Upon completion of the reaction the resultant mixture was diluted with H₂O to give the desired product as a precipitate that was collected using

vacuum filtration and washed with H₂O. Yield 80%; M.P. 245.9-247.4 °C; ¹H NMR (400 MHz, DMSO-*d*₆) δ: 11.05 (1H, s), 9.29 (1H, d, *J* = 1.7), 8.81 (1H, dd, *J* = 4.8, 1.6), 8.71 (1H, d, *J* = 8.5), 8.55-8.52 (2H, m), 8.46 (1H, dt, *J* = 7.9, 1.8), 8.21 (1H, d, *J* = 8.0), 7.87 (1H, dd, *J* = 8.4, 7.4), 7.62 (1H, dd, *J* = 7.3, 4.8), 4.03 (2H, t, *J* = 7.4), 1.68 (2H, app. sext, *J* = 7.4), 0.94 (3H, t, *J* = 7.4). ¹³C NMR (100 MHz, DMSO-*d*₆) δ: 166.06, 164.07, 163.51, 152.66, 149.70, 136.36, 131.86, 131.37, 131.26, 130.95, 128.98, 126.77, 123.95, 122.60, 122.47, 118.31, 41.60, 21.37, 11.88.

3-(1,3-Dioxo-2-propyl-2,3-dihydro-1*H*-benzo[*de*]isoquinolin-6-yl carbamoyl)-1-(4-fluorobenzyl)-pyridinium bromide 4 (NapNic)

The above nicotinamide **3** (100 mg, 0.28 mmol) and 4-fluorobenzyl bromide (35 μL, 0.28 mmol) were dissolved in CH₃CN (50 mL) under N₂. The reaction mixture was heated for 18 h then cooled to room temperature. The solution was then concentrated to one-third of its original volume using a rotary evaporator and on standing at room temperature the product precipitated as a light yellow-coloured solid. The solid was collected by vacuum filtration, washed with diethyl ether (10 mL) then air dried. Yield 84%; MP 155.7-156.8 °C; ¹H NMR (500 MHz, DMSO-*d*₆) δ: 11.41 (1H, s), 9.85 (1H, s), 9.37 (1H, d, *J* = 6.0), 9.24 (1H, d, *J* = 8.0), 8.70 (1H, d, *J* = 8.5), 8.60 (2H, m), 8.40 (1H, t, *J* = 7.2), 8.19 (1H, d, *J* = 8.0), 7.93 (1H, t, *J* = 8.0), 7.74 (2H, dd, *J* = 8.1, 5.5), 7.35 (2H, m), 5.99 (2H, s), 4.04 (2H, t, *J* = 7.1), 1.08 (2H, app. sext, *J* = 7.4), 0.95 (3H, t, *J* = 7.4). ¹³C NMR (100 MHz, DMSO-*d*₆) δ: 163.91, 163.43, 162.25, 161.95, 147.08, 145.89, 145.18, 132.21, 132.13, 131.66, 131.63, 130.73, 130.70, 130.56, 128.84, 128.68, 127.34, 126.36, 123.21, 122.93, 116.76, 116.54, 63.35, 41.71, 21.34, 11.87. HRMS (ESI, m/z, positive ion) for C₂₈H₂₃FN₃O₃⁺ [M]⁺ calc. 468.1723; found 468.1721; HRMS (ESI, m/z, negative ion) for C₂₈H₂₃⁷⁹BrFN₃O₃ [M-H]⁻ calc. 546.0907; found 546.0823 and C₂₈H₂₃⁸¹BrFN₃O₃ [M-H]⁻ calc. 548.0886; found 548.0804.

S2 Spectra of new compounds

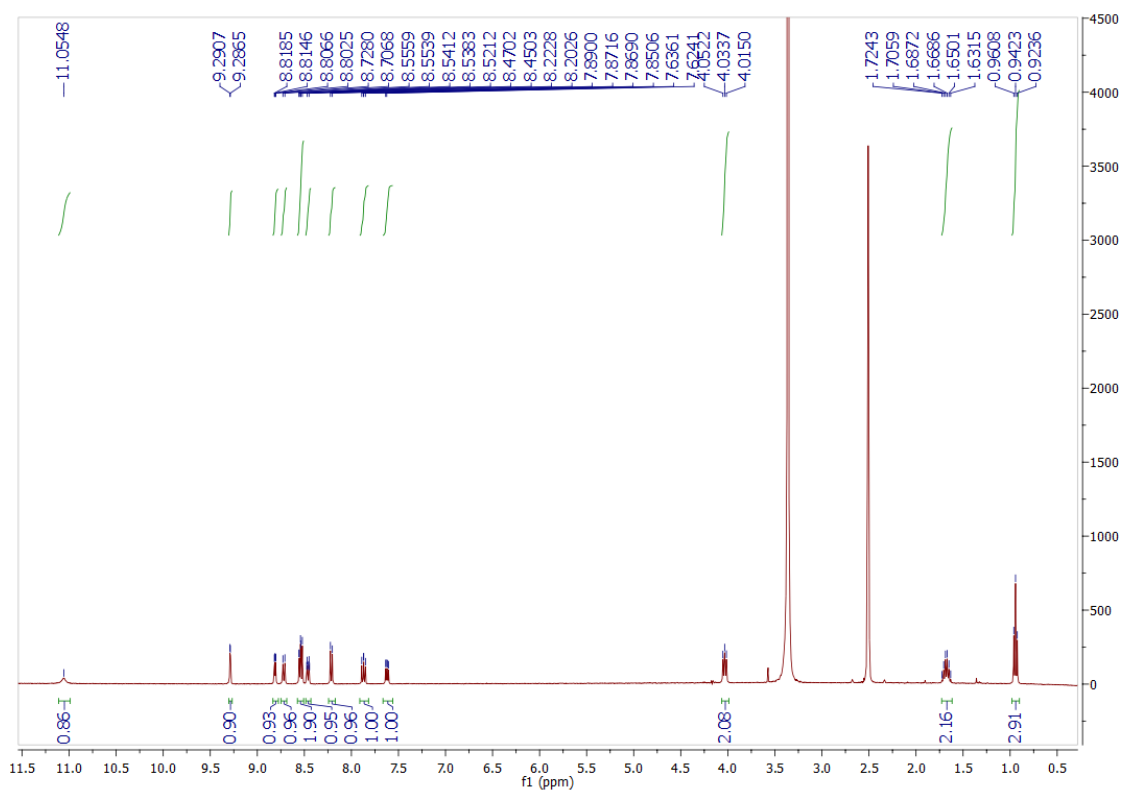


Figure S1. ^1H NMR spectrum of **3** in $\text{DMSO-}d_6$.

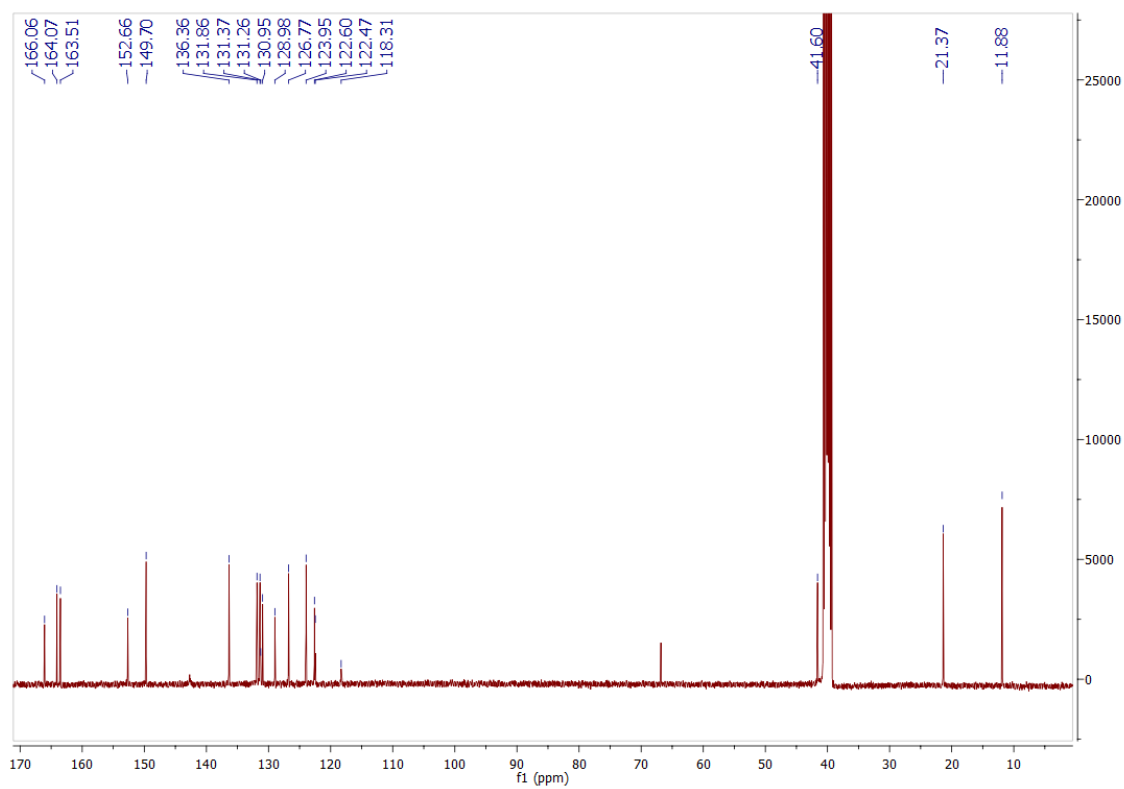


Figure S2. ^{13}C NMR spectrum of **3** in $\text{DMSO-}d_6$.

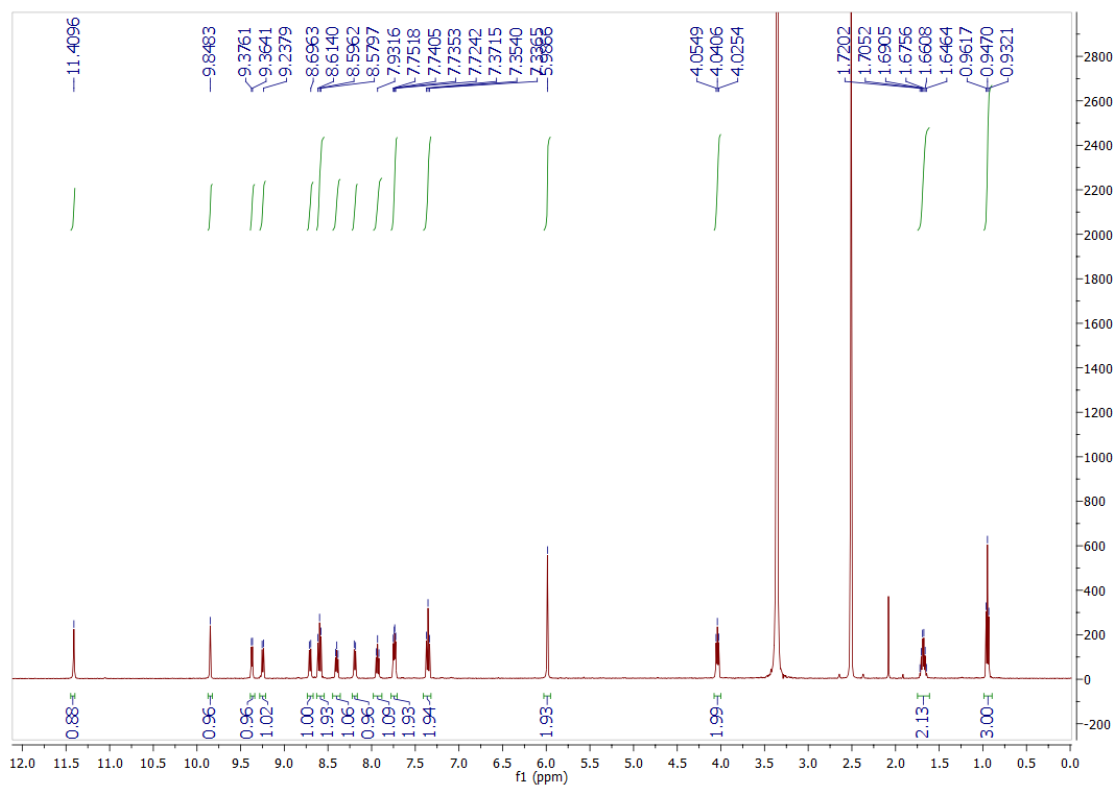


Figure S3. ^1H NMR spectrum of **4** (NapNic) in $\text{DMSO-}d_6$.

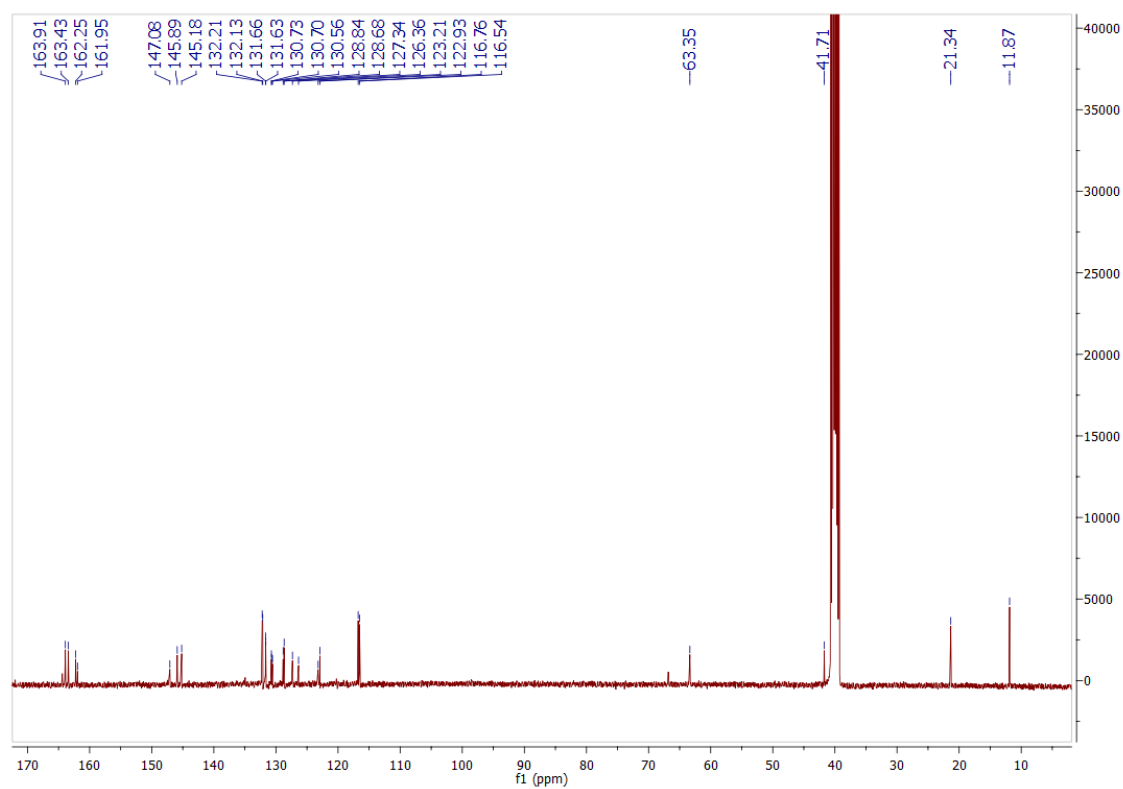


Figure S4. ^{13}C NMR spectrum of **4** (NapNic) in $\text{DMSO-}d_6$.

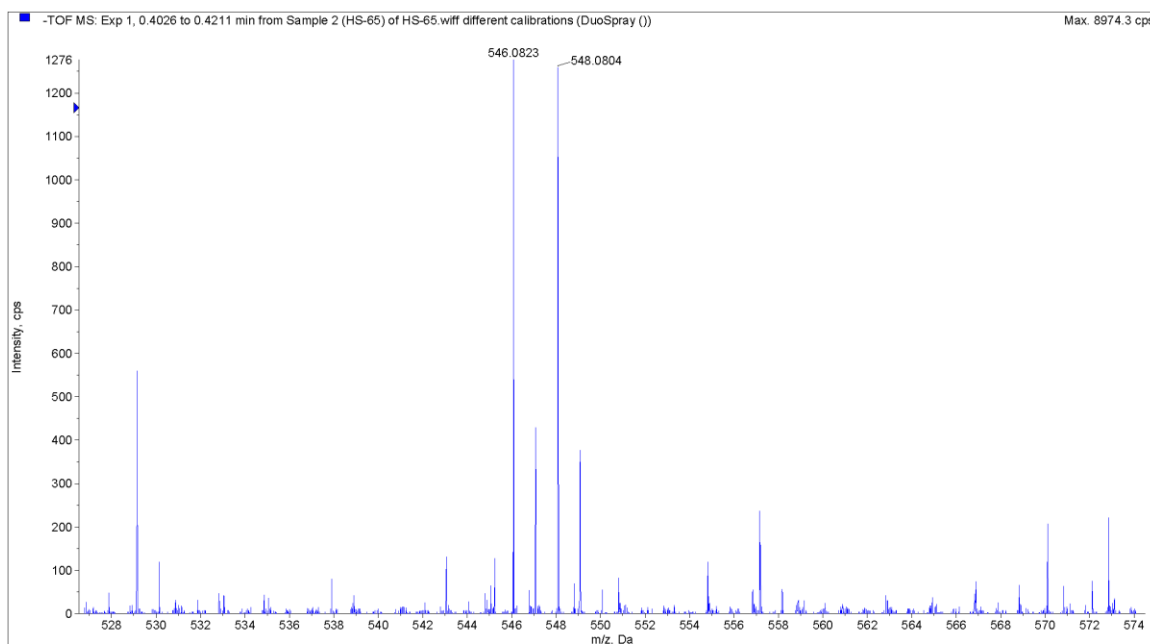


Figure S5. Mass spectrum (negative ion mode) of **4 (NapNic)**.

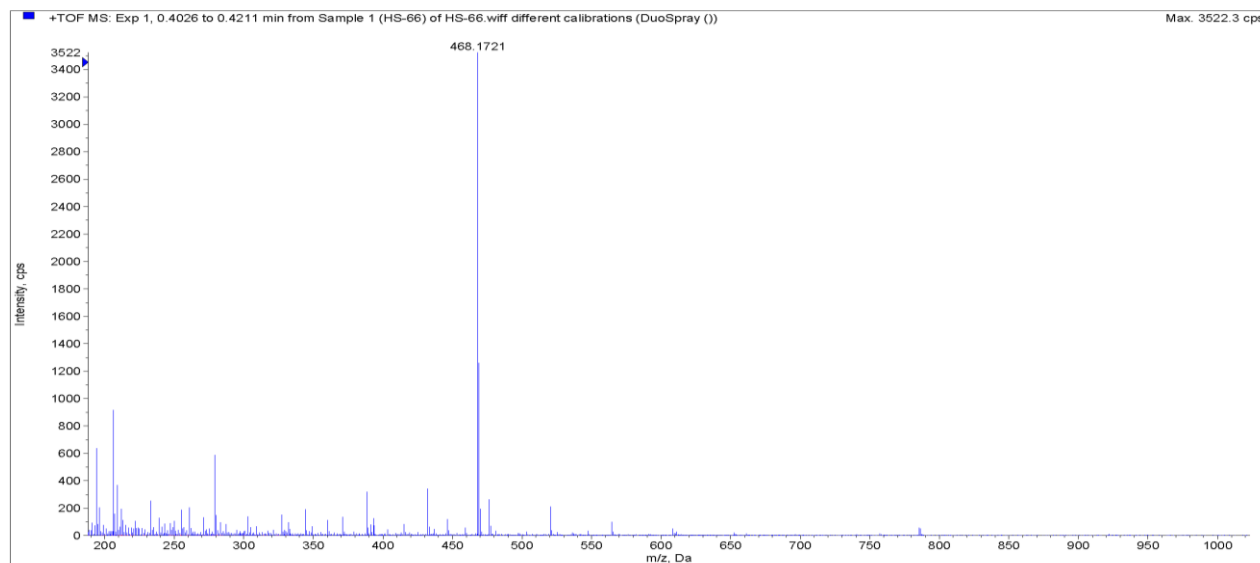


Figure S6. Mass spectrum (positive ion mode) of **4 (NapNic)**.

S3. UV-vis and fluorescence spectroscopy experiments

The absorption studies were recorded on a Cary 300 UV-visible spectrophotometer and Cary eclipse fluorescence spectrophotometer was used for emission spectra using 10 mm quartz cell with 10 nm slit width. All measurements were performed at room temperature 25 ± 2 °C in phosphate buffer (10 mM, pH 7.4) with solutions shaken well before recording any spectrum. The reduction reaction was performed through addition of $\text{Na}_2\text{S}_2\text{O}_4$ into the solution of the probe and latter was re-oxidised with H_2O_2 . The redox reversibility of the probe was investigated through addition of $\text{Na}_2\text{S}_2\text{O}_4$ followed by H_2O_2 for the indicated times.

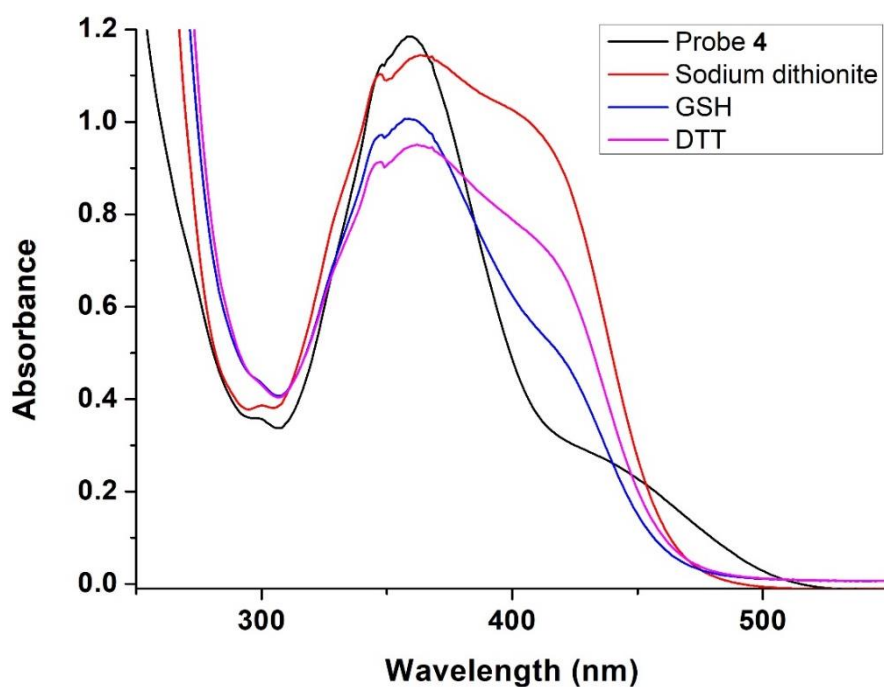


Figure S7. Absorption spectra of **4** (NapNic) (10 μM) before and after reaction with reducing agents $\text{Na}_2\text{S}_2\text{O}_4$ (500 μM), glutathione (400 μM) and dithiothreitol (DTT, 400 μM). All solutions were prepared in phosphate buffer (10 mM, pH 7.4).

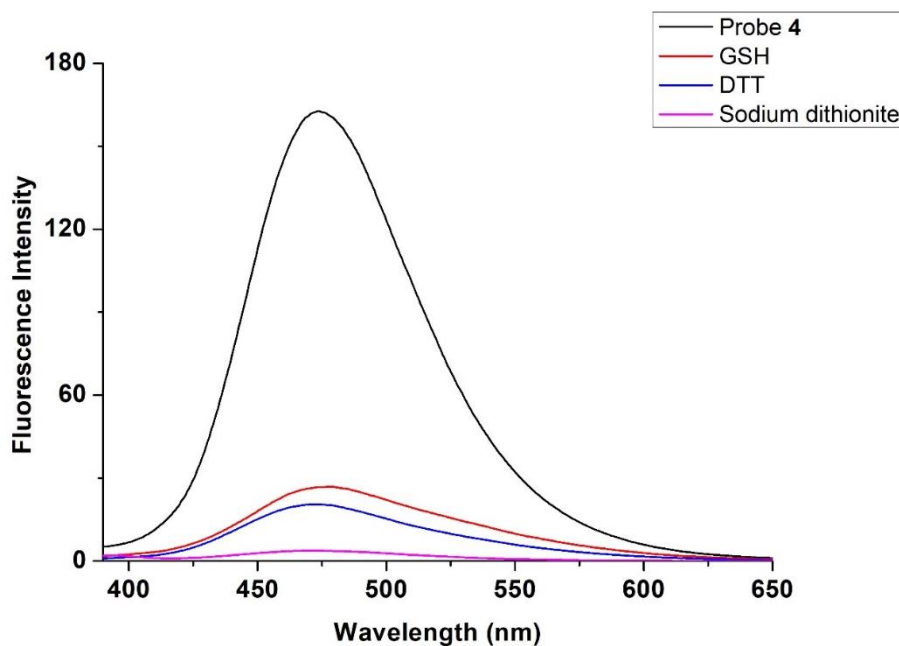


Figure S8. Emission spectra of **4** (NapNic) (10 μM , $\lambda_{\text{exc}} = 360 \text{ nm}$) before and after reaction with of reducing agents $\text{Na}_2\text{S}_2\text{O}_4$ (500 μM), glutathione (400 μM) and dithiothreitol (DTT, 400 μM). All solutions were prepared in phosphate buffer (10 mM, pH 7.4).

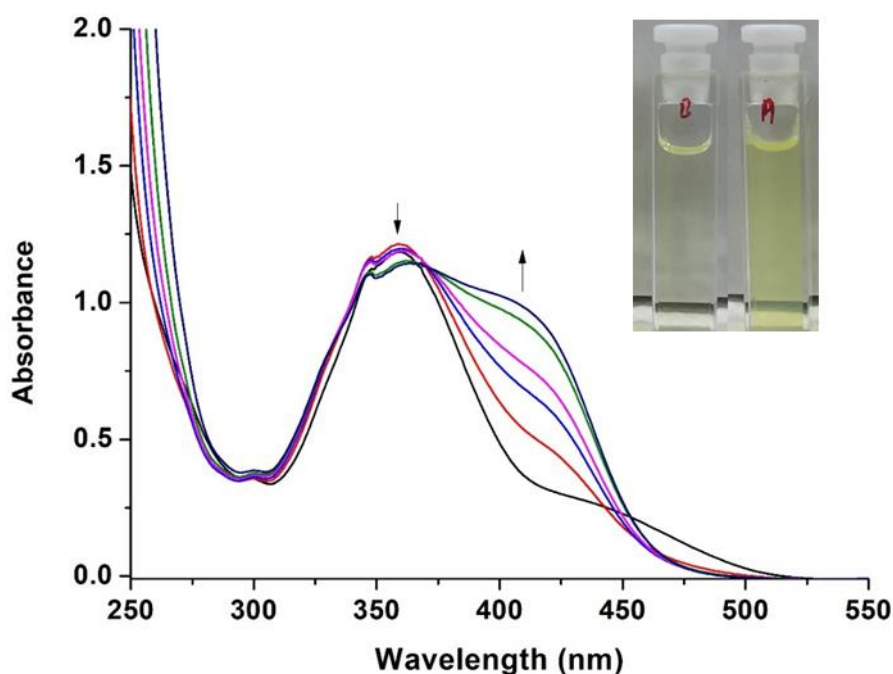


Figure S9. Change in the absorption spectra of **4** (NapNic) (10 μM) with the incremental addition of $\text{Na}_2\text{S}_2\text{O}_4$ (0-500 μM) in phosphate buffer (10 mM, pH 7.4). Inset: Change in colour of **4** (NapNic) from cuvettes under white light with (left) no $\text{Na}_2\text{S}_2\text{O}_4$ and (right) after addition of 500 μM $\text{Na}_2\text{S}_2\text{O}_4$.

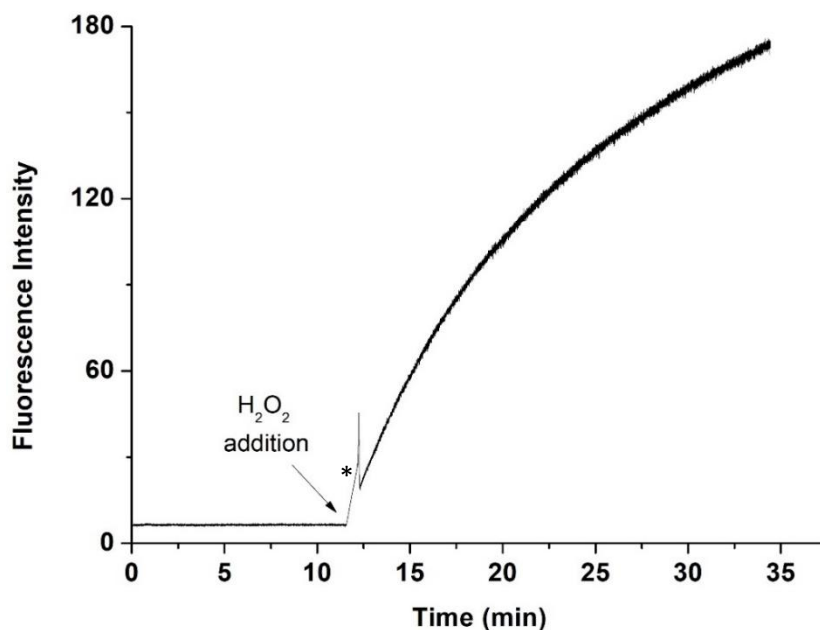


Figure S10. Change in the fluorescence intensity of the reduced form of **4** (NapNic-H) (10 μM , $\lambda_{\text{ex}} = 360 \text{ nm}$) in phosphate buffer (10 mM, pH 7.4) at 474 nm upon addition of H_2O_2 (1 mM in phosphate buffer 10 mM, pH 7.4). * The slight noise in the graph resulted from the physical addition of H_2O_2 to the cuvette.

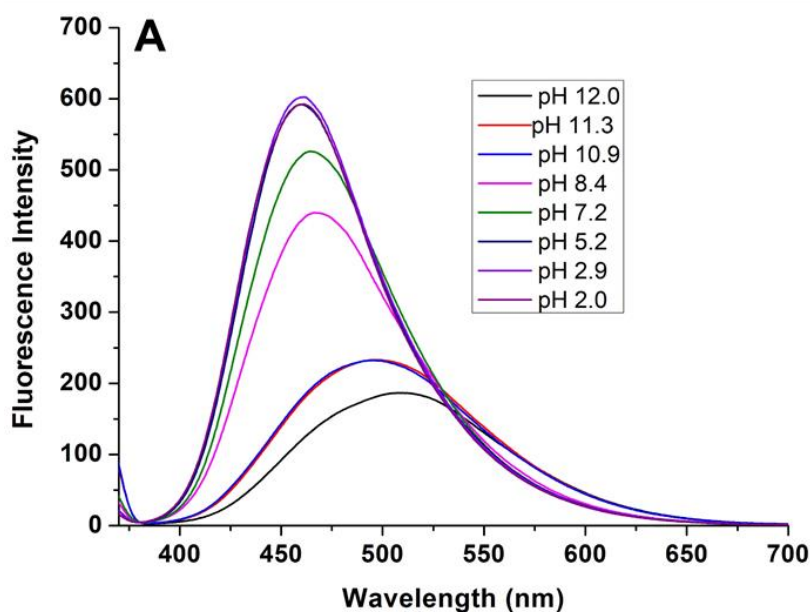


Figure S11. Change in the fluorescence of **4** (NapNic) (10 μM , $\lambda_{\text{ex}} = 360 \text{ nm}$) in acidic and basic media. The change in emission at elevated pH is typical for 4-amidonaphthalimides.³ Dilute solutions (0.1 M) of both HCl and NaOH were used to adjust pH.

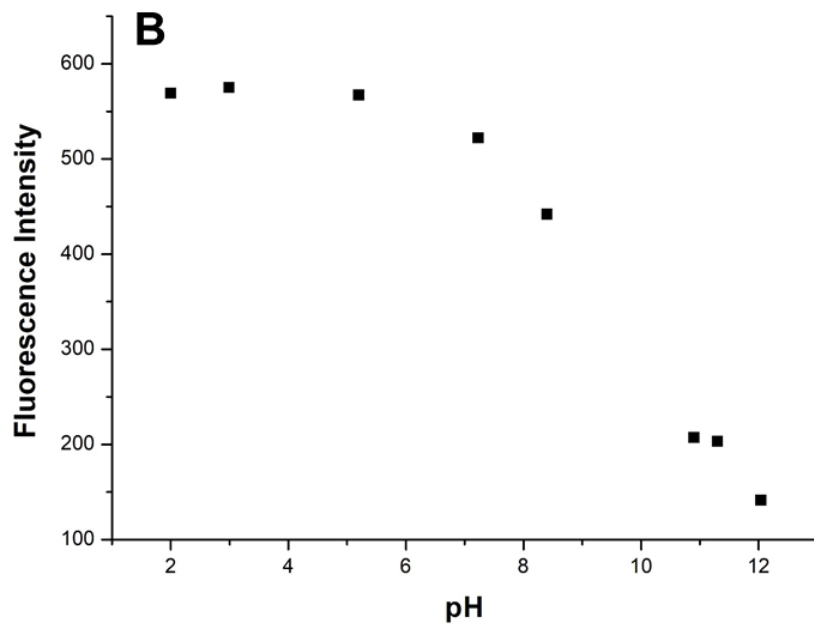


Figure S12. Change in the fluorescence intensity of **4** (NapNic) (10 μ M) at 470 nm in acidic and basic medium. Dilute solutions (0.1 M) of both HCl and NaOH were used to adjust pH.

S4 Electrochemistry

Electrochemical measurements were collected on an ER466 Integrated Potentiostat System. A single cell compartment consisting of a glassy carbon working electrode, a platinum wire auxiliary electrode and a silver wire reference electrode was used. Cyclic voltammogram experiments were performed using a 1 mM solution of the analyte (**NapNic**) in acetonitrile, with 0.1 M tetrabutylammonium hexafluorophosphate as the supporting electrolyte and ferrocene/ferrocenium as an internal standard. Scans were performed at a rate of 100 mVs⁻¹ with the solutions degassed with argon prior to each measurement. Measurements were converted to a standard hydrogen electrode reference (vs. SHE) for comparison with the literature.

S5 Additional ^1H NMR experiments

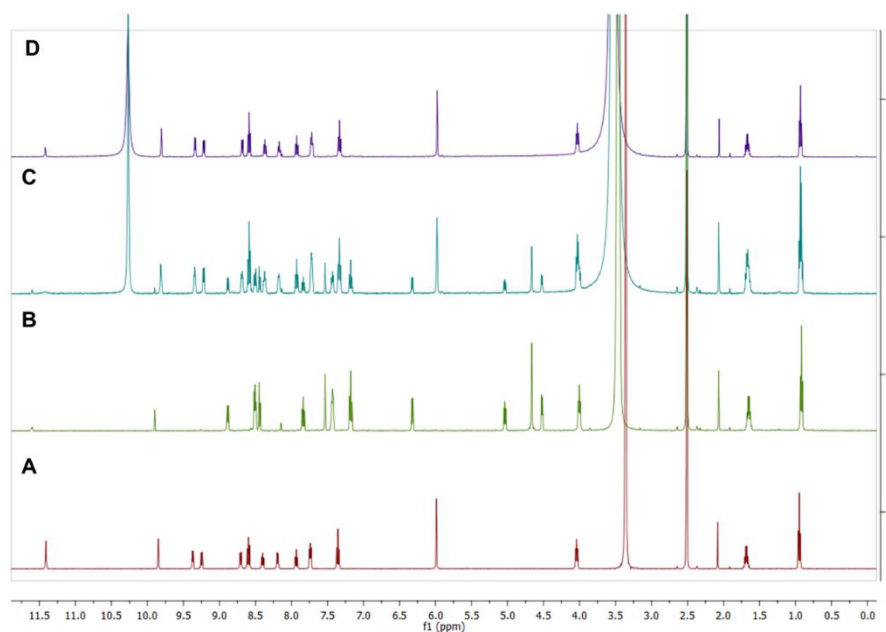


Figure S13. ^1H NMR spectra of (a) oxidised probe **4** in DMSO-d_6 , (b) reduced probe **4** using sodium dithionite, (c) re-oxidised probe **4** using H_2O_2 (15 min after addition) and (d) re-oxidised probe **4** using H_2O_2 (6 h after addition). The probe was reduced using 50 equiv. of $\text{Na}_2\text{S}_2\text{O}_4$ and the spectrum immediately recorded. This was followed by addition of 100 equiv. of H_2O_2 and spectra (c) and (d) were recorded after 15 min and 6 h respectively. The broad singlet at $\delta = 10.27$ was assigned to H_2O_2 (confirmed by recording the ^1H NMR spectrum of H_2O_2 in DMSO-d_6 shown in figure S14 below).

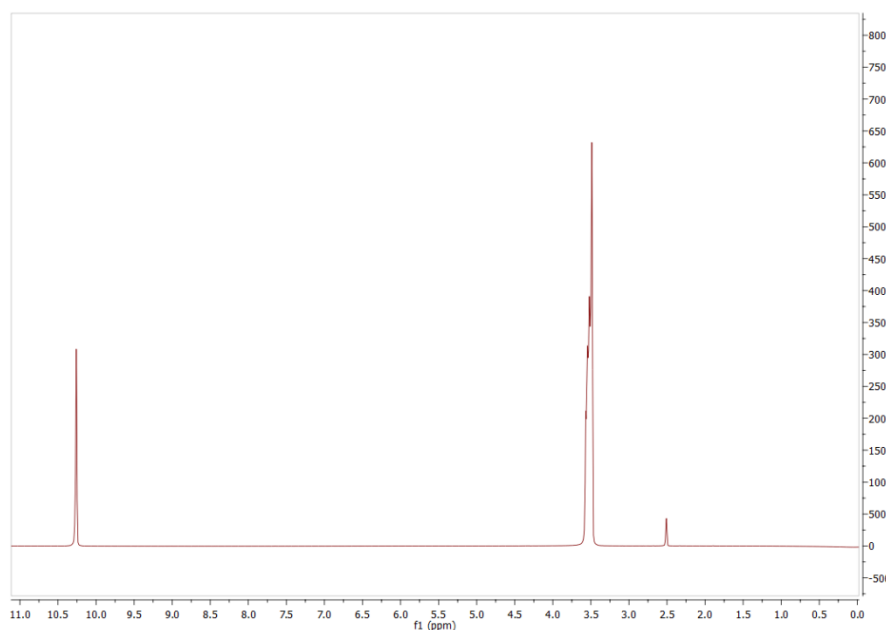


Figure S14. ^1H NMR spectra of H_2O_2 in DMSO-d_6 .

S6 Imaging studies

Human basal epithelial A549 lung adenocarcinoma cells were used for cellular studies. Cells were maintained in exponential growth as monolayers in Advanced Dulbecco's Modified Eagle's Medium (ADMEM) supplemented with 2% (v/v) foetal bovine serum (FBS) and 1% (v/v) glutamine (G). Cells were incubated at 37 °C in 5% (v/v) CO₂ under humidified conditions. The A549 cell line was maintained at a passage number below 25 and sub-cultured twice a week using trypsin with 0.25% EDTA to dislodge cells from the flask.

For confocal microscopy, A549 cells were seeded in 35 mm glass bottom MatTek® dishes at a cell-density of 3×10^5 cells and allowed to adhere overnight. Cells were dosed with 35 µM solutions of **NapNic** in ADMEM (supplemented with 2% FBS, 1% G) for 30 min and then washed twice with phosphate-buffered saline (PBS), and imaged in FluoroBrite™ DMEM media (supplemented with 2% FBS, 1% G). Hydrogen peroxide, dithionite (DTT) and *N*-acetylcysteine were added from PBS stocks to final concentrations of 50 µM.

Colocalisation studies were performed by incubating cells simultaneously with 50 µM **NapNic** and 50 µM Nile Red in ADMEM (supplemented with 2% FBS, 1% G) for 30 min. Cells were then washed twice with PBS, and then imaged in FluoroBrite™ DMEM media (supplemented with 2% FBS, 1% G). Confocal images were acquired using an Olympus Fluoview FV3000 inverted microscope and a UPLSAPO 60WX water-immersion objective lens (Numerical Aperture = 1.2) equipped with Tokai Hit stage top incubator and lens heater to maintain 37 °C. Excitation light at 405 nm (5% laser power) was provided by a 405 nm OBIS laser. Images were acquired with the Olympus FV31S-SW viewer software (v2.3.1.163) and analysed using ImageJ FIJI (1.52p, Java 1.8.0_172) with colocalisation plugins.

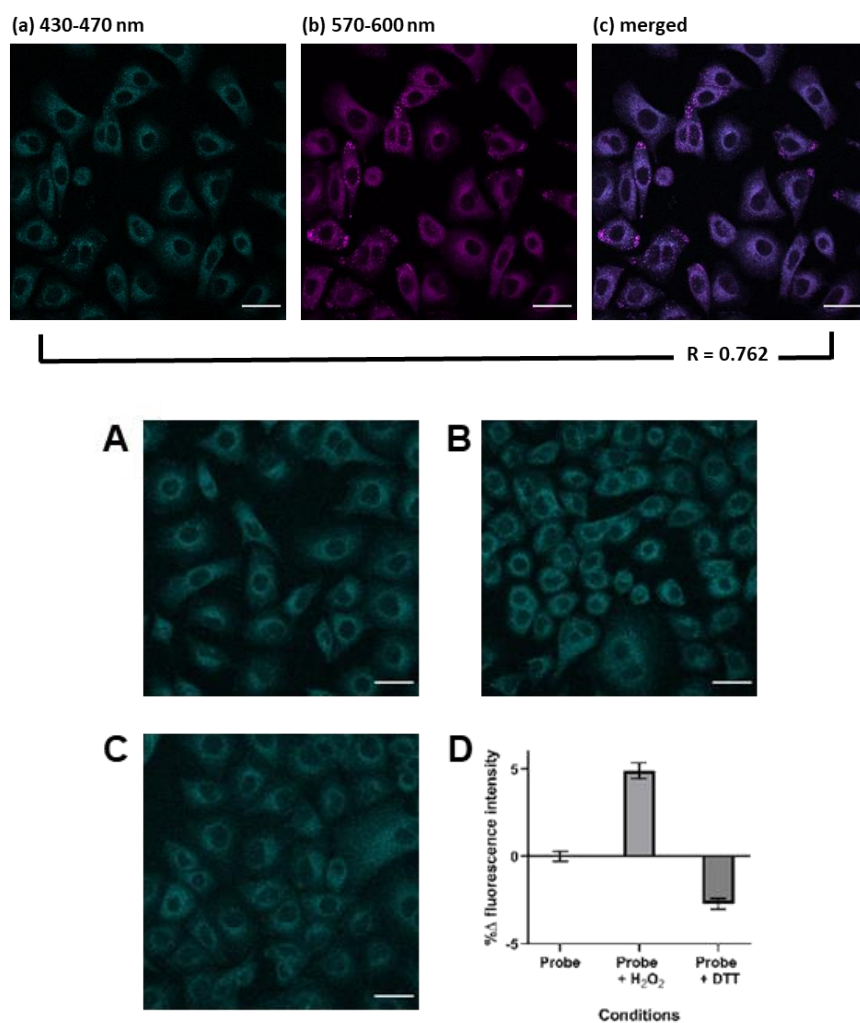


Figure S15: *TOP:* Confocal microscopy images of A549 cells stained with **NapNic** (50 μ M, 30 min) and Nile Red (50 μ M, 30 min): (a) channel 1 (430 – 470 nm) (b) channel 2 (570 – 670 nm) (c) merged images of channel 1 and 2. Purple regions represent colocalisation of **NapNic** with Nile Red, with a Pearson’s coefficient of $R = 0.762$ with Nile Red. Scale bars represent 30 μ m. *BOTTOM:* Representative micrographs of A549 cells treated with (A) **NapNic** only (35 μ M, 30 min), (B) **NapNic** (35 μ M, 30 min) followed by H_2O_2 (50 μ M, 30 min) and (C) **NapNic** (35 μ M, 30 min) followed by sodium dithionite (50 μ M, 30 min). Micrographs shown were maximum projections of z-stacked confocal images. All scale bars represent 30 μ m. (D) Mean fluorescence intensities were measured from cells imaged across 3 different fields of view per experiment for each condition. Data were presented as fold change in fluorescence intensities compared to the fluorescence intensities of cells treated with probe only. Error bars represent the standard error of the mean fold change (S.E.M.) across 3 experiments; $N = 3$ independent experiments.

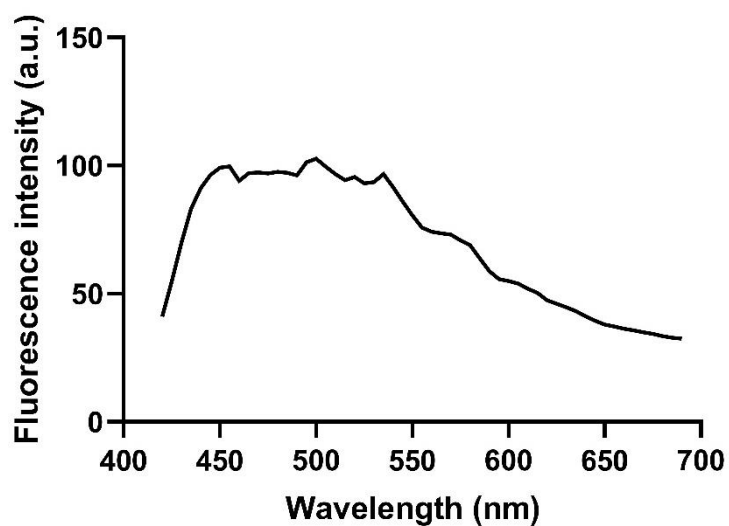


Figure S16: The fluorescence spectral scan of **NapNic** (35 μM) measured from A549 cells. A 405 nm laser was used as the laser source and fluorescence emission was collected from 410 – 700 nm with a band width of 20 nm and a step size of 5 nm.

S7 Comparison of NapNic with related probes

The new **NapNic** compares favourably with related probes from the literature⁴⁻¹¹ as it possesses the necessary features of water solubility, high Stokes shift, global selectivity and a significant change in fluorescence intensity on “switching”.

The clear illustration of the structural reversibility of **NapNic** obtained using ¹H NMR titration techniques is unique amongst related probes.

Name	Solvent	Selectivity	$\lambda_{\text{ex}}/\lambda_{\text{em}}$ (nm)	Fluorescence response
Lyso-NI-se ⁴	CH ₃ CN:H ₂ O 1:1 v/v	HOCl	430/540	22 fold increase
Lyso-NHS ⁵	CH ₃ CN:PBS 1:9 v/v	H ₂ S	450/555	42 fold increase
Cy-O-Eb ⁶	HEPES buffer	GSH/H ₂ O ₂	768/794	8 fold increase
NpFR1 ⁷	HEPES buffer	Global	405/545	125 fold increase
NpFR2 ⁸	HEPES buffer	Global	488/545	115 fold increase
[Ru(byp) ₃ ²⁺]-PTZ ⁹	Phosphate buffer	ClO ⁻ /H ₂ S	480/605	47 fold increase
L1 ¹⁰	Phosphate buffer	HOCl	405/505	n.a.
NDMTC ¹¹	Phosphate buffer:EtOH 1:1 v/v	HOCl	410/547	n.a.
NapNic	Phosphate buffer	Global	360/474	82 fold increase

References

- 1 W. A. Carole and T. J. Colacot, *Chem. – A Eur. J.*, 2016, **22**, 7686–7695.
- 2 T. N. Konstantinova, P. Meallier and I. Grabchev, *Dyes Pigm.*, 1993, **22**, 191–198.
- 3 K. N. Hearn, T. D. Nalder, R. P. Cox, H. D. Maynard, T. D. M. Bell, F. M. Pfeffer and T. D. Ashton, *Chem. Commun.*, 2017, **53**, 12298–12301.
- 4 Z. Qu, J. Ding, M. Zhao and P. Li, *J. Photochem. Photobiol. A Chem.*, 2015, **299**, 1–8.
- 5 T. Liu, Z. Xu, D. R. Spring and J. Cui, *Org. Lett.*, 2013, **15**, 2310–2313.
- 6 K. Xu, M. Qiang, W. Gao, R. Su, N. Li, Y. Gao, Y. Xie, F. Kong and B. Tang, *Chem. Sci.*, 2013, **4**, 1079–1086.
- 7 J. Yeow, A. Kaur, M. D. Anscomb and E. J. New, *Chem. Commun.*, 2014, **50**, 8181–8184.
- 8 A. Kaur, K. W. L. Brigden, T. F. Cashman, S. T. Fraser and E. J. New, *Org. Biomol. Chem.*, 2015, **13**, 6686–6689.
- 9 F. Liu, Y. Gao, J. Wang and S. Sun, *Analyst*, 2014, **139**, 3324–3329.
- 10 B. Zhang, X. Yang, R. Zhang, Y. Liu, X. Ren, M. Xian, Y. Ye and Y. Zhao, *Anal. Chem.*, 2017, **89**, 10384–10390.
- 11 B. Zhu, P. Li, W. Shu, X. Wang, C. Liu, Y. Wang, Z. Wang, Y. Wang and B. Tang, *Anal. Chem.*, 2016, **88**, 12532–12538.